OMTN, Volume *11*

Supplemental Information

Generation of *Hutat2:Fc* Knockin Primary Human Monocytes Using CRISPR/Cas9

Bowen Wang, Jiahui Zuo, Wenzhen Kang, Qianqi Wei, Jianhui Li, Chunfu Wang, Zhihui Liu, Yuanan Lu, Yan Zhuang, Bianli Dang, Qing Liu, Wen Kang, and Yongtao Sun

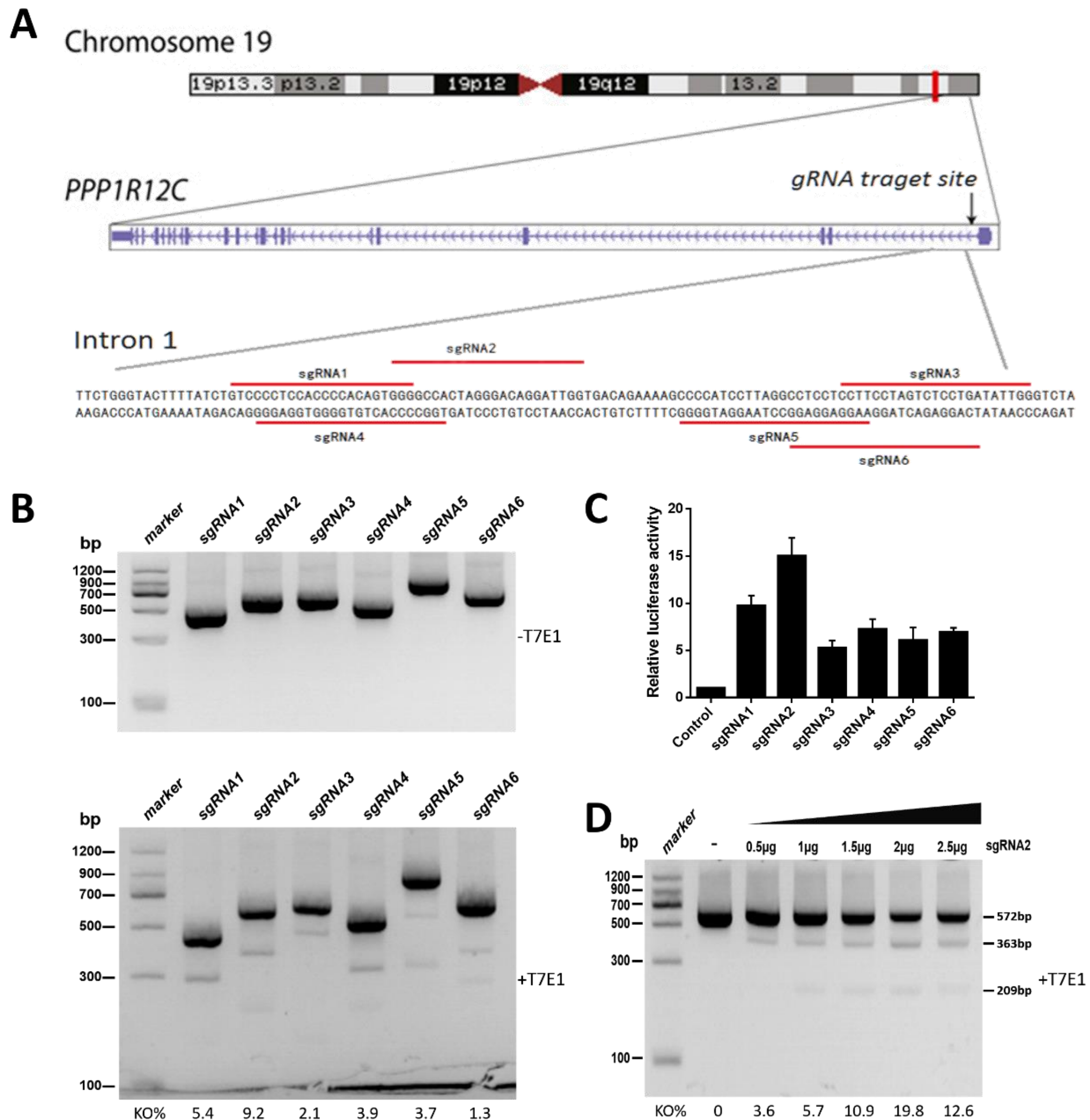

Figure S1. Evaluation of the knock-out efficiency of sgRNA1-6 targeting the *AAVS1* locus in HeLa cells. (A) Schematic of sgRNA1-6 designed to target the *AAVS1* locus. (B) Detection of the knock-out efficiency of sgRNA1-6 using a T7E I assay. Amplicons of sgRNA1-6 that were treated with T7E I (+T7E I) or without T7E I (-T7E I) were separated by 2% agarose gel electrophoresis. DSB sites were recognized and digested by T7E I. Undigested and digested bands were consistent with the predicted sizes from the *AAVS1* locus. The knock-out frequencies were calculated and are shown below the gel. (C) Comparison of the relative luciferase activity of sgRNA1-6 by a universal CRISPR activity assay (n=3). (D) As in *B*, the knock-out efficiency of sgRNA2 in HeLa cells was evaluated by T7E I assays with a dose gradient. The results are presented as the means from independent experiments. The error bars denote the s.e.m.

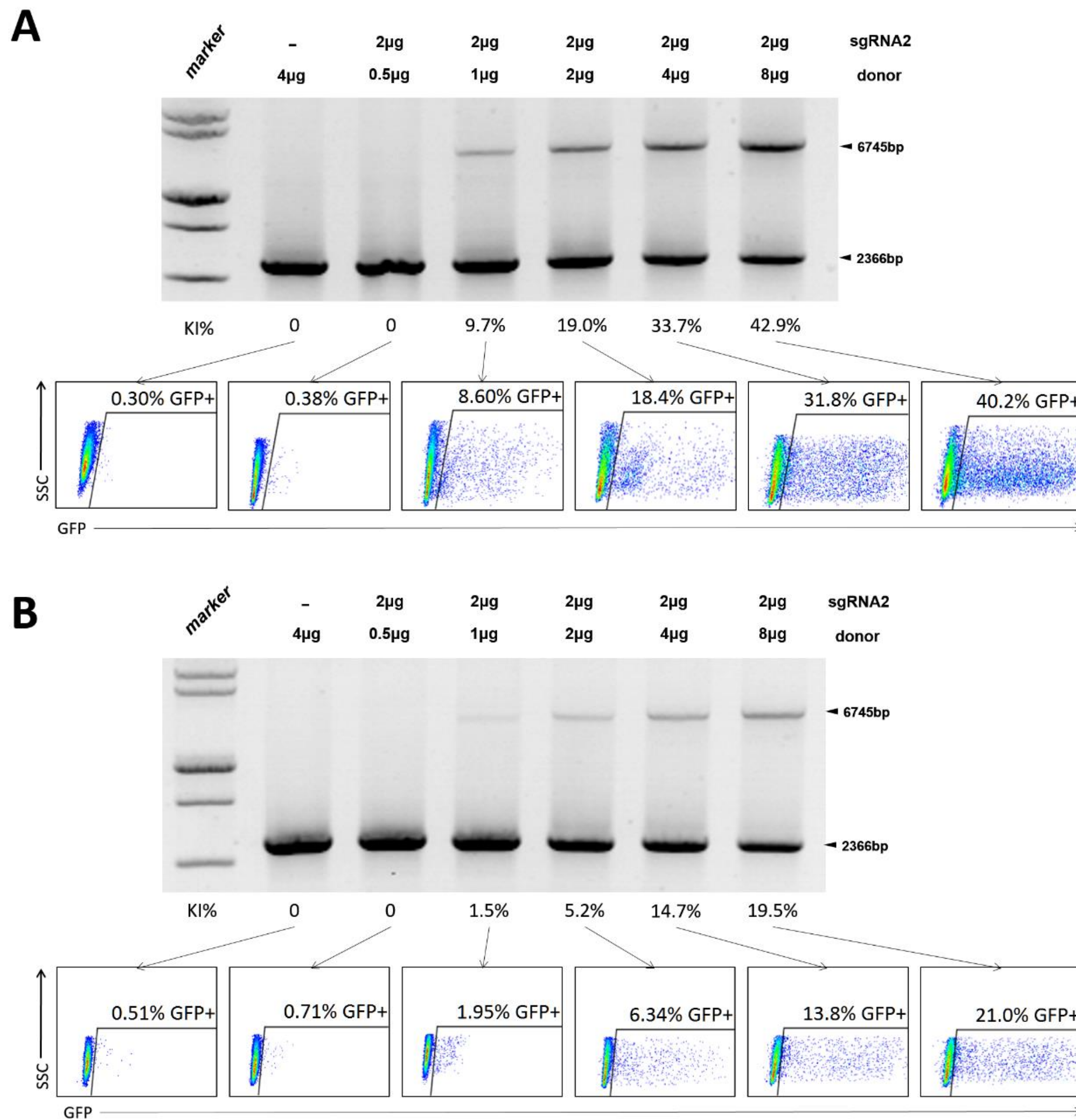

Figure S2. CRISPR-mediated KI of *Hutat2:Fc* gene fragments into the *AAVS1* locus in 293 T and U937 cells. (A) As in Figure. 1E, following selection with Puro, PCR using the primers GT-F/GT-R was performed to semi-quantitatively analyze the KI efficiency in 293 T cells which transfected with different ratios of sgRNA2 to donor plasmids. The editing frequencies were confirmed by FACS. (B) As in *A*, transduction was conducted by electroporation in U937 cells without selection.

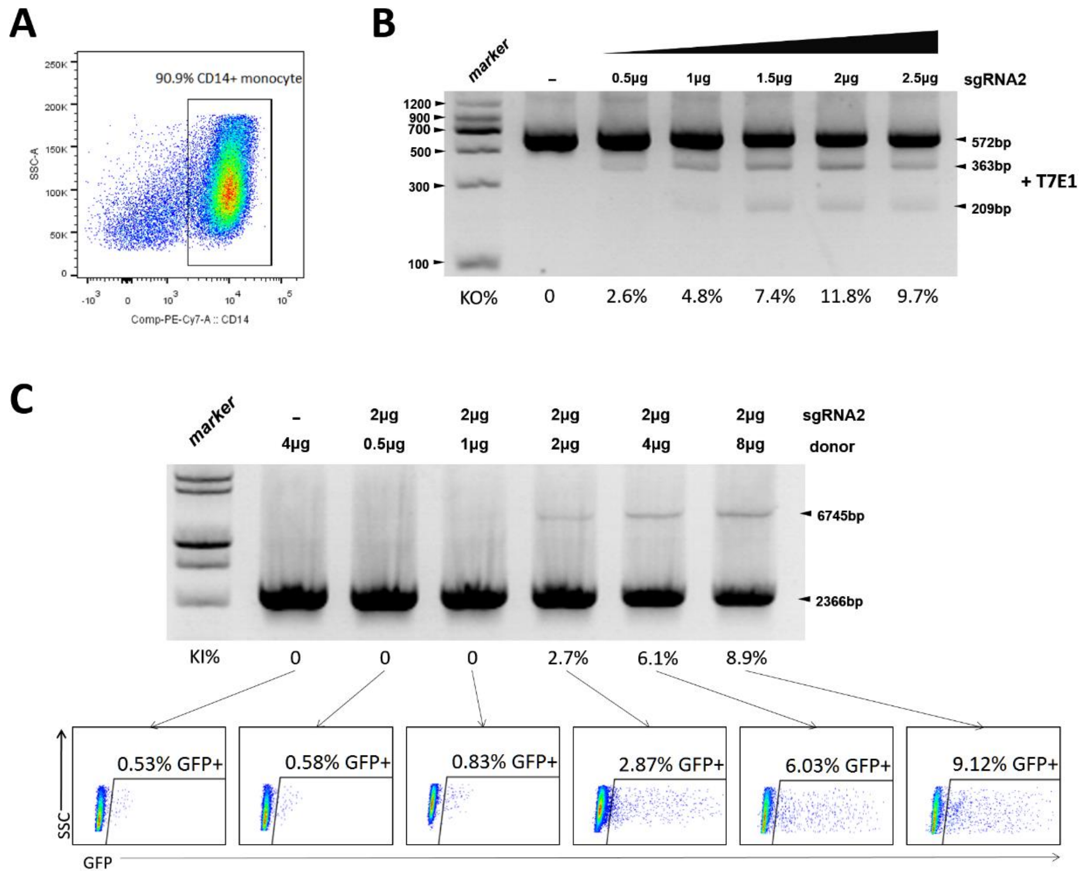

Figure S3. CRISPR-mediated KI of *Hutat2:Fc* gene fragments into the *AAVS1* locus in human primary monocytes. (A) Representative FACS plots of human primary monocytes sorted from PBMCs and counterstained by PE/Cy7-CD14. (B) As in Fig. S1D, the knock-out efficiency of sgRNA2 in monocytes was evaluated by T7E I assays with a dose gradient. (C) As in Figure. S2B, transduction was conducted by electroporation in monocytes without selection.

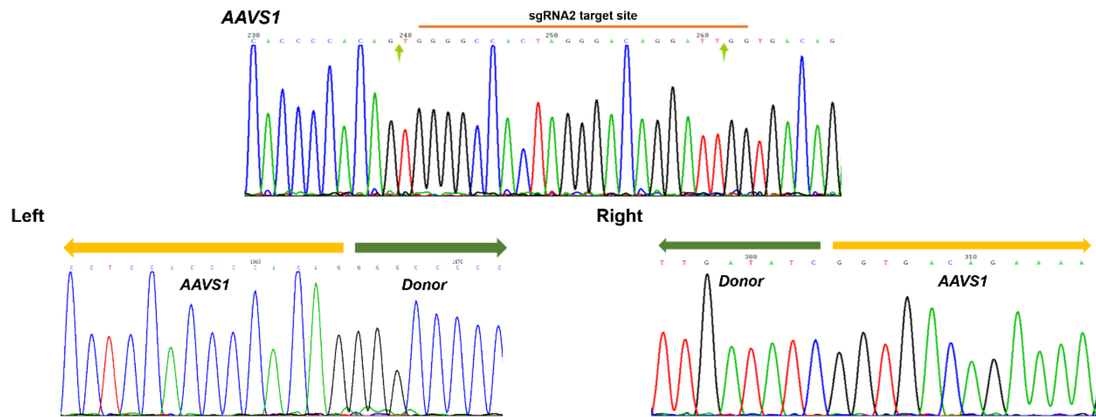

Figure S4. Confirmation of *Hutat2:Fc* insertion into the *AAVS1* locus by Sanger sequencing. PCR amplicons encompassing the sgRNA2 target site were subjected to Sanger sequencing. The normal control sequence is presented above. Green arrows indicate the insertion sites on both sides of sgRNA2. The expected DNA bases at both boundaries of genome-donor and donor-genome were presented below to confirm the full-length insertion of donor templates.

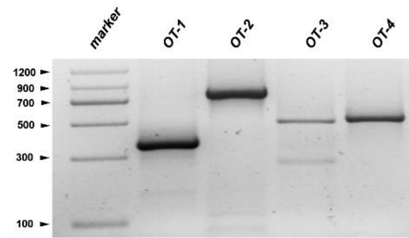

Figure S5. Analysis of the potential off-target effects of sgRNA2. The sgRNA2-mediated off-target sites OT1-4 were predicted and analyzed by T7E I assays. Off-target mutation was found in OT-3.

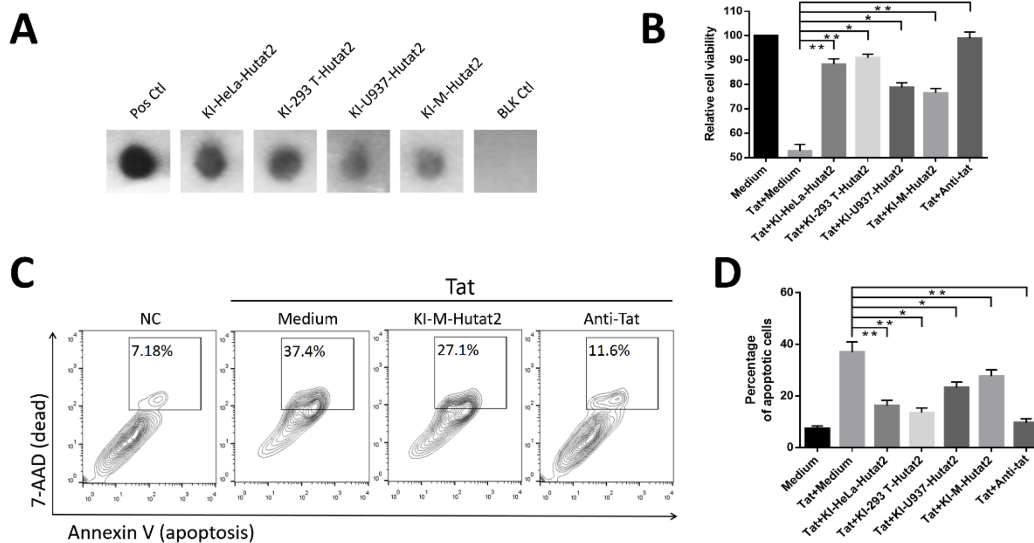

Figure S6. Evaluation of the binding ability of secreted Hutat2:Fc to HIV-Tat and the protective effects of Hutat2:Fc against Tat-mediated neurotoxicity in HTB-11 cells. (A) The biological binding of Hutat2:Fc from conditioned media was evaluated through DIBA assays. Commercial anti-Tat antibodies were used as a positive control. Tat dilution without antibody incubation was used as a black control. (B) The relative cell viability of HTB-11 after treatment with or without each type of conditioned media was determined through CCK8 assays (n=6). (C) Representative flow cytometer images gated on apoptotic cells (Annexin V^+ and 7-AAD^+) after exposure to HIV-Tat in the presence or absence of KI-M-Hutat2. Commercial anti-Tat antibodies were used as a positive control. (D) Percentage of apoptotic cells from C after treatment with or without each conditioned media (n=6). Dunnett's t test was used to perform statistical analyses of the data shown in B and D; $*P<0.05$, $**P<0.01$. The results are presented as the means from independent experiments. The error bars denote the s.e.m.

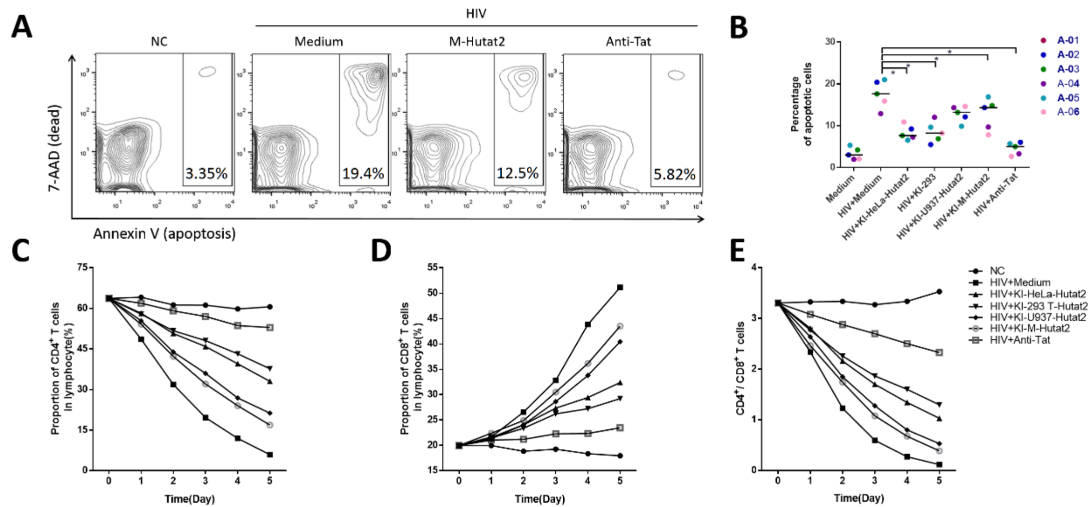

Figure S7. Effects of secreted Hutat2:Fc on the apoptosis of PBMCs and recovery of T cells. (A) Representative flow cytometer images gated on apoptotic cells (Annexin V^{+} and 7-AAD^{+}) and dying cells (Annexin V ^{bright} and 7-AAD $^{dim/-}$) after exposure to HIV-1Ba-L in the presence or absence of KI-M-Hutat2. (B) Percentage of apoptotic cells from *A* after treatment with or without each conditioned media (n=6). Wilcoxon matched-pairs signed-ranks test was used to perform the statistical analyses; **P*<0.05, ***P*<0.01. (C-E) Proportion of CD4+, CD8+ and CD4+/CD8+ T cells after exposure to HIV-1Ba-L with or without each conditioned media (n=6). The results are presented as the medians from independent experiments.

Table S1. Oligonucleotides for sgRNAs, off-targets and primers used for PCR

Target name	Sequences (5'-3')	
sgRNA1	GTCCCCTCCACCCCACAGTGGGG	
sgRNA2	GGGGCCACTAGGGACAGGATTGG	
sgRNA3	CCTTCCTAGTCTCCTGATATTGG	
sgRNA4	TGGCCCCACGTTGGGGTGGAGGG	
sgRNA5	AAGGAGGAGGCCTAAGGATGGGG	
sgRNA6	TCAGGAGACTAGGAAGGAGGAGG	
Off-target name	Sequences (5'-3')	Location
OT-1	GGGACCATCAGGGACAGGATGGG	chr6:+36765462
OT-2	GGGGCCAGTAGGGAGAGGATAGG	chr16:-32037124
OT-3	GGGGCCAATTAGGACAGGATGGG	chr13:+106612910
OT-4	GGGGCCAGTGGGGACAGGAAGGG	chr2:-232824535
PCR primers	Sequences (5'-3')	Production size
F-sgRNA1	CCCCACTGTGGGGTGGAGGGGAC	444bp
R-sgRNA1	TCTGGTGACACACCCCCATTTC	
F-sgRNA2	GAGGATGGAGAGGTGGCTAAAGCC	572bp
R-sgRNA2	AGAGCTTGGCAGGGGGTGGGAGG	
F-sgRNA3	CTTTGGGGTTGTCCAGAAAAACGG	590bp
R-sgRNA3	AGAGAGGATCCTGGGAGGGAGA	
F-sgRNA4	TCCAGGCAAAGAAAGCAAGAGG	512bp
R-sgRNA4	TTTGCTTACGATGGAGCCAGA	
F-sgRNA5	GAAACGAGAGATGGCACAGGCCCC	806bp
R-sgRNA5	GCGGCCGTCTGGTGCGTTTCACT	
F-sgRNA6	TGAGAGGTGACCCGAATCCAC	619bp
R-sgRNA6	GCGGCCGTCTGGTGCGTTTCACTG	
F-OT-1	GATGGATAGGTGAGTCAGCCAG	369bp
R-OT-1	ACATTCGTTGATACTCGTAAAACAC	
F-OT-2	CGGTGAACTCTTGGGAGACC	745bp
R-OT-2	GCAGTCGGAGGAAGTGACAA	
F-OT-3	CGTGACTCCCGAAAAGCCT	497bp
R-OT-3	GCCTCGGCTGGGTCAAG	
F-OT-4	GCCTCGGCTGGGTCAAG	524bp
R-OT-4	GTGCCCGTATCCAGAGTG	
PCR primers	Sequences (5'-3')	
GT-F	GTCGACTTCCCCTTCCGATGTTG	
Ai3-2737F	GAGCCTCTGCTAACCATGTTC	
Neo-F	CGCATTGTCTGAGTAGGTGTC	
Ai3-2781R	GCACAATAACCAGCACGTTG	
Puro-GT-R	GCAACAGATGGAAGGCCTCCTGGCG	
GT-R	GAAACTGGCCGGGAATCAAGAGTCA	